Polyimide Probes for Contact-Mode SPM Subsurface Thermal Imaging Applications

Angelo Gaitas, PicoCal Inc. and University of Michigan, Ann Arbor, USA

BIOGRAPHY

Angelo Gaitas is the president and CEO of PicoCal Inc. and a research associate in the Electrical Engineering and Computer Science Department at the University of Michigan, Ann Arbor. He received an MBA from the University of Wisconsin, Madison, and an MS in solid-state physics from the University of London. His research interests span a variety of scanning probe microscope techniques for manufacturing applications.

ABSTRACT

This article describes the results obtained with a surface micromachined probe for scanning thermal microscopy. The probe uses polyimide as the structural material and an embedded thin-film metal resistor as the sensing element. The typical dimensions of a probe are 250 µm in length, 50 µm in width, and 3-10 µm in thickness. The probe has measured spring constant less than $0.1\ \mathrm{N\ m^{-1}}$, and about 40 Ω nominal resistance. It offers a tip diameter of 100 nm. The probe was used to map the spatial variation in thermal conductance of various test samples. Surface and subsurface characteristics were observed.

KEYWORDS

scanning probe microscopy, atomic force microscopy, scanning thermal microscopy, microthermal analysis, polymers, failure analysis, nanoscience, nanotechnology

ACKNOWLEDGEMENTS

The author would like to thank Prof. Yogesh Gianchandani, Dr Song Xu and Dr Shamus McNamara for their valuable contributions to this paper, and Sematech for providing samples.

AUTHOR DETAILS

Angelo Gaitas,
PicoCal Inc.,
PO Box 131490,
Ann Arbor, MI 48113-1490, USA
Tel: +1 734 913 2608
Email: angelo@picocal.com

Microscopy and Analysis 20(2):S11-S14 (UK), 2006

INTRODUCTION

Thermal measurements at the nanometer scale are of both scientific and industrial interest. Over the past decade, scanning microscopy using thermally sensitive probes has been used in a variety of applications. For instance, scanning thermal microscopy (SThM) has been used for ultralarge-scale integration (ULSI) lithography research and cellular diagnostics in biochemistry [1-3], detecting parameters such as phase changes in polymer blends [4], Joule heating [5], for measuring material variations in semiconductor devices [6], and subsurface imaging of metal particles [4]. Furthermore, SThM has been used to perform near-field photothermal microspectroscopy [8]. Finally, it has been used for data storage and many other applications [9-11].

Various thermal probes have been developed since the invention of scanning thermal microscopy by Williams and Wickramasinghe in 1986 [12]. These probes are generally made from thin dielectric films on a silicon substrate and use a metal or semiconductor film bolometer to sense the tip temperature. Other approaches, using more involved micromachining methods, have also been reported [13]. In a bolometer probe, such as the one used in this study, the resistor is used as a local heater and the fractional change in probe resistance is used to detect the temperature and/or the thermal conductance of the sample [14].

Thermal probes are used to map the spatial variation in thermal conductance of various test samples whose subsurface variations are not detectable topographically. This article presents a preliminary study of subsurface imaging on copper wires using a polyimide thermal probe. The ultimate goal of this effort is to address the semiconductor industry's challenge to develop non-destructive in-line viewing of copper voids. The use of SThM holds significant promise to detect defects such as voids in copper lines in advanced complementary metal oxide semiconductor (CMOS) processes. Since copper interconnects are common in advanced CMOS devices, it is vital for the semiconductor industry to obtain timely information about the quality of the copper electroplating process and related steps.

The use of non-electrical inspection methods for copper electroplating has several limitations. Because copper is opaque, optical inspection methods are difficult. In addition, since most of these failures occur on the interior of the copper trace, their detection is also difficult with topographic measurement methods using an atomic force microscope (AFM) or scanning electron microscope (SEM). While electrical methods are accurate, they require at least two points of contact and special geometries that permit access to both ends of the trace to be measured; this access is usually not available without special test structures. Another option, thermal measurement methods, can potentially overcome the problems posed by optical, AFM, SEM or electrical test methods. Such techniques measure the interior of the copper trace, enabling the non-destructive localized detection of voids in the copper. Thermal measurements require only a single point of contact and permit inspection of all the copper traces, regardless of geometry. Vias may be inspected because the barrier layer or remaining dielectric material have a much higher thermal resistance compared to copper.

Scanning thermal probes fabricated by six- to seven-mask surface micromachining processes using polyimide as the cantilever

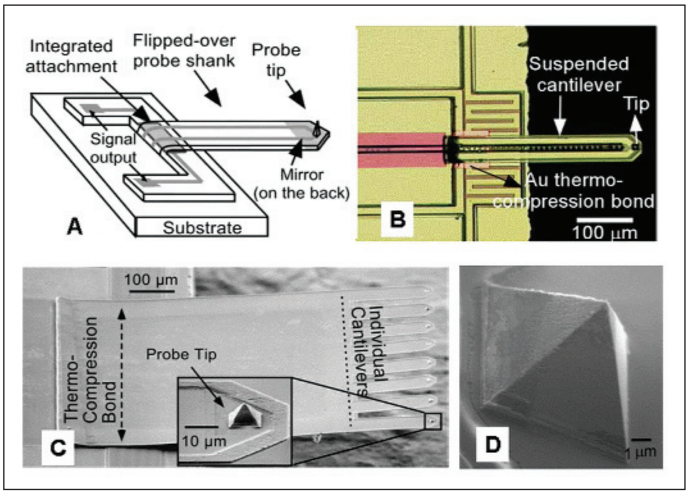

Figure 1:
(A) Schematic of the probe die including the probe cantilever and tip. Reprinted from [1] with permission.
(B) Scanning electron microscope image of the probe. Reprinted from [1] with permission.
(C) SEM image of an eight-probe array . Reprinted from [20] with permission.
(D) SEM image of a tip.

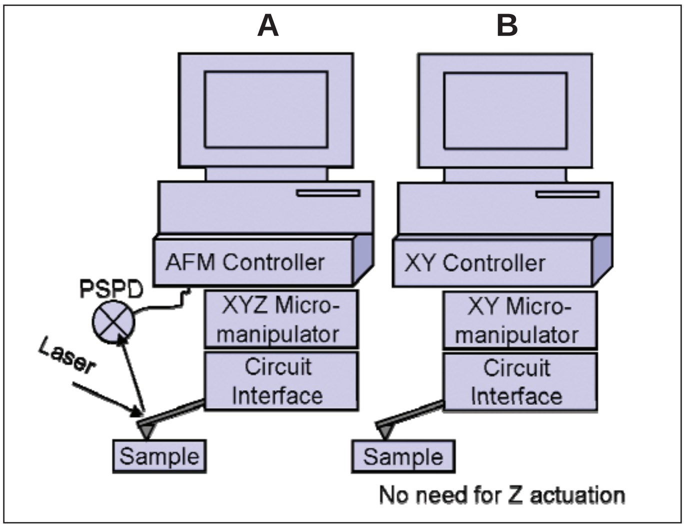

Figure 2:
Comparison of original AFM imaging mode (A) and a simpler system for thermal measurements in which Z-axis actuation is eliminated (B).

material have been previously reported [1,2,14,15]. These probes have been used for temperature mapping and subsurface imaging [15], for microcalorimetry applications to measure the glass transition temperature in a photoresist [1,2,14], and for maskless submicrometer thermochemical patterning of photoresists [16]. Hendatro *et al*. [17] used the probes for the detection of hot-spots in integrated circuits (IC) revealing that the highest amplitude of thermal waves generated by an operating nMOSFET (n-type metal-oxide semiconductor field-effect transistor) is located at a region close to the drain area. Basu *et al*. [19] have been using the probes for microfluidics-related work, namely for high-speed liquid pumping, mixing and particle entrapment in thin layers of oil and water. The probes have been arrayed into a multi-probe system for higher throughput large area scanning [20]. An eight-probe array, such as the one in Figure 1C, has been used to produce composite thermal images of various commercial ICs. Finally, the probes were used for high-speed contact mode topography achieving rates of 48 Hz (1.47 mm s^{-1}) and for lateral force scans, suggesting that polyimide is a more suitable structural material for cantilevers used in lateral force measurements [21].

MATERIALS AND METHODS

Structure and fabrication

The structure of the polyimide probe is shown in Figure 1. The probe tip diameter used was less than 100 nm but the probe tip can be further reduced to below 50 nm with oxide sharpening. The probe had a topographical resolution of <1 nm and a spring constant of <0.1 N m^{-1}. The tip height was 8 µm, and the cantilever's dimensions were 250 µm × 50 µm × 3 µm. The cantilever material was polyimide with an embedded thin wire of Cr/Au, which also served as a sensing element. The tip was also made of Cr/Au. The probe had spatial resolution of less than 100 nm. Thermal conductance changes of the order of 3 pW K^{-1} have been measured. A comparison with a Wollaston wire thermal probe is presented in Table 1.

The probes were microfabricated in a seven-masking step sequence. Initially, a mold for the tip was created by anisotropic wet etching on a Si(100) substrate. Then a sacrificial layer was deposited and patterned, followed by the lower polyimide and the metals. Later, the second polyimide layer was deposited and patterned, followed by a gold layer, which was used for thermocompression bonding and served as a mirror. Finally, the probe was released, flipped over, and held in place by a thermocompression bond.

Interface circuit and setup

There are many methods by which a thermal probe may be utilized. It can be operated in a passive manner whereby the tip temperature attains the localized sample temperature. In order to map the thermal conductance of samples, the probe is typically operated at an elevated temperature. The varying heat loss is monitored by its effect on the tip through the sample to the chuck below, which is held at room temperature. The simplest interface circuit operates in approximately constant power mode where an open-loop interface circuit is used to gauge the probe resistance change (thermal conductance change), which can be calculated from the output voltage change. The interface circuit includes a Wheatstone bridge, gain stages, and filters to reduce noise. The output voltage is plotted for the thermal image. In the case of thermal conductance contrast mapping, the change in probe resistance is proportional to the change in output voltage. The supplied power change is equal to the conductive heat loss between the tip and sample, which is proportional to the change in the thermal conductance of the sample. Thus the change in output voltage represents the thermal conductance contrast of the sample [1].

Alternatively, the scanning thermal probe may be operated at a constant tip temperature and the power required to keep the temperature constant is measured (closed-loop mode – feedback required). This method permits contrast imaging and thermal conductivity measurements to be performed. When the Wheatstone bridge comes out of balance, an instrumentation amplifier amplifies the change in voltage. Subsequently, the change in voltage is fed into a proportional-integral (PI) controller that provides a compensation current to keep the bridge balanced. The average probe temperature increases or decreases with the compensation power, so that the probe resistance is adjusted by a compensation current through the PI controller until the change in voltage is zero. By increasing the temperature control resistance, the probe resistance is also increased.

An AC thermal dither may be applied to the probe to improve thermal resolution or to perform thermal capacitance measurements. The thermal resolution is improved by filtering the signal through a bandpass filter to reduce the noise level. Since the thermal wave generated is an evanescent wave, the AC thermal dither may be used to control the effective probe depth. Higher frequencies of operation reduce the effective probe depth.

AFM systems for thermal probes

The probes may be operated with an AFM system. The thermal information from the probes was fed to a circuit module such as the one described above, which in return interfaced with an AFM controller (Figure 2A). In these measurments the probe was operated in contact mode by scanning a thermal probe tip across the sample and making measurements at discrete points. Thermal probes operated in contact mode show improved performance. By contrast, operation in a tapping or non-contact mode has several disadvantages. First, the temperature sensitivity of the probe is compromised because of the large thermal

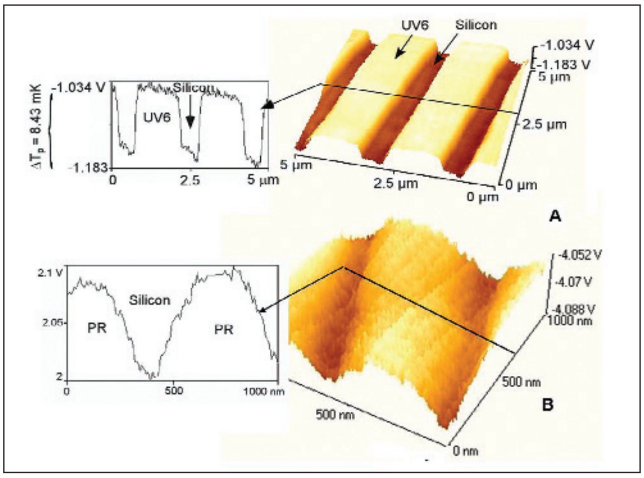

Figure 3:
AFM images taken without Z-direction feedback.
(A) Scans of a developed UV6 photoresist. The photoresist pattern is 350-nm thick and 500-nm wide. Reprinted from [1] with permission.
(B) Map of thermal conductance of a developed PMMA photoresist on a 4-inch silicon wafer. The photoresist pattern was 240-nm thick and 200-nm wide with a pitch of 400 nm. Reprinted from [22] with permission.

Performance	Wollaston wire probe	Polyimide probe
Tip diameter	1 µm	<100 nm
Topographical resolution	NA	<1 nm
Temperature resolution	2.5 K	<10 mK
Thermal conductance	<0.23 µW K^{-1}	<3 pW K^{-1}
Normal spring constant	1-5 N m^{-1}	0.1 N m^{-1}

Table 1:
Comparison of characteristics of a Wollaston wire probe [7] and the polyimide thermal probe.

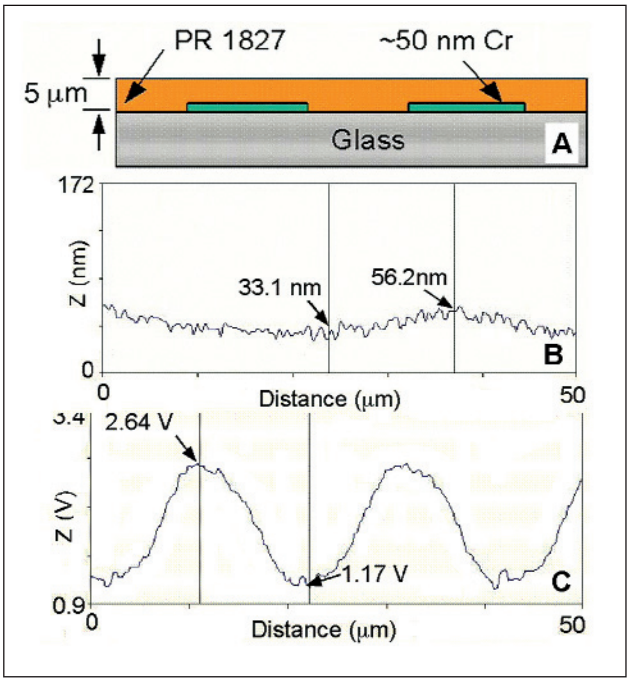

Figure 4:
(A) Schematic of a glass substrate with 50-nm thick Cr lines covered by 5 µm of photoresist.
(B) An AFM scan shows very little topographical variation.
(C) The Cr lines are clearly visible with a thermal probe scan. Reprinted from [15] with permission.

resistance of the air gap. Second, spatial resolution is reduced because the effective sensing area is enlarged as the distance between the sensor and the sample increases. Third, high stiffness in the probe is required which may cause damage to soft samples. The use of polyimide probes eliminates these problems.

Moving on from the original approach, a simpler system has been devised (Figure 2B), which obtains only thermal information and does not require Z-axis feedback. The high compliance of the probe allows scans of samples with large topographic variations. An X-Y stage controls the position of the probe while an interface circuit is used between the data acquisition computer and the thermal probe. A simple construction is enabled by eliminating Z-axis actuation and the hardware that is needed for it, such as photodetectors, lasers, and other electronics. An additional advantage is that the probes can be arrayed for high-throughput large-area scanning (Figure 1C).

RESULTS AND DISCUSSION

SPM scans

Figure 3 contains scan images obtained without contact force feedback control using the system described above and depicted in Figure 2B. Scans of a developed Shipley UV-6 deep ultraviolet photoresist made without Z-direction feedback are shown in Figure 3A. The photoresist pattern was 350 nm thick and 500 nm wide. Comparing the line profiles with and without Z-direction feedback, the with-feedback operation provided higher signal-to-noise ratios. The fluctuation of the tip-sample contact area was larger without feedback. Figure 3B shows a thermal conductance map of developed polymethylmethacrylate (PMMA) on a four-inch silicon wafer. The photoresist pattern was 240-nm thick and 200-nm wide with a pitch of 400 nm. The scan results showed that the thermal probe can provide a spatial resolution better than 200 nm without contact-force feedback control [22].

Subsurface imaging capability is very useful for measuring semiconductor devices where multiple layers are present and the final IC is coated with a passivation layer. Thermal images showing metal lines through a passivation layer were obtained. Results demonstrating the subsurface imaging capability of the thermal probe are shown in Figure 4. A sample containing 50-nm thick chromium lines on a glass substrate was coated with a 5-µm thick planarized photoresist, which had a thermal resistivity of 0.193 W m^{-1} K^{-1} (Figure 4A). A topographical image of the sample showed that the photoresist was uniform and the underlying Cr layers were not detected (Figure 4B). The thermal image, on the other hand, clearly detected the underlying Cr layers. The variation in thermal resistance amounted to a 1% change in 1.0 × 10^{10} K W^{-1} and the signal-to-noise ratio was in excess of 15, as shown in Figure 4C [15].

Figure 5 illustrates another example of subsurface mapping. The sample contained 90-nm wide Cu lines covered with 250 to 300-nm wide and 125-nm thick natural oxide. An SEM picture of the trench before Cu deposition is shown in Figure 4A. An SEM picture of a Cu line is shown in Figure 5B. An AFM scan of the Cu lines covered with a thick layer of oxide is shown in Figure 5C. Figures 5D and 5E illustrate overlays of thermal scans superimposed on topographical scans and show <300 nm discontinuities in thermal conductance maps occurring under the natural oxide. These discontinuities were not visible topographically. The images revealed subsurface information about the Cu lines, which potentially may be related to Cu voids. The current through the probe was 12 mA and the nominal probe resistance was 26 Ω. The area scanned was 6 × 6 µm^2 and the scan rate was set at 1 Hz for Fig. 5D and 1.4 Hz for Fig. 5E.

Simulations

Numerical simulations were performed in order to demonstrate the feasibility of detecting voids in copper lines and to enhance understanding of the quality and detectability of the thermal conductance signal. Thermal scans over copper lines having various types of voids with different sizes and locations were simulated using the Femlab 3 Multiphysics Modeling package by Comsol [23]. Each simulation yielded maps of the change in thermal conductance as an area the size of the probe-tip heated the surface of the simulated copper lines.

The simulated structure was based on Intel's 130-nm process [24]. The structure consisted of a 400-nm thick lower layer of field oxide, the bottom of which was held at 0°C. The top layer was a dielectric, 280-nm thick, 1-µm wide, and 1-µm long, with a copper feature, 150-nm wide, 150-nm long, and 280-nm thick, located at the center of the dielectric. A void was simulated in the copper layer and its location and size were varied. A cylindrical thermal probe with 50-nm diameter resided on top of the copper and the probe temperature was held at 100°C at the point of contact with the copper.

Simulations of features with and without voids were performed and the heat flux out of the thermal probe was calculated. The number of bits of resolution in the sensed signal required in order to detect a particular void was determined from the difference in thermal resistance with and without a void for a particular depth. The simulations confirmed that voids in closer proximity to the surface and larger voids were easier to detect. The simulations also indicated that the minimum number of bits of resolution required to detect most voids was within the performance levels of the scanning thermal microscopy system. For example, a 100-nm diameter void at 140-nm depth would require 8-bit resolution to be detected, while a 140-nm diameter void at the same depth would require 6 bits, and a 40-nm diameter void would require 12 bits. In Figure 6, the X axis represents the ratio of void depth to void diameter and the Y axis the bits required to detect a particular void. The two lines represent 70-nm and 140-nm depths. At a fixed depth, the bits required to detect a void decrease as the void size increases.

CONCLUSIONS

This article has reviewed a surface micromachined scanning thermal probe that uses polyimide as the structural material and an embedded thin-film metal resistor as the sensing element. The probe tip offers a diameter <100 nm, a topographical resolution of <1 nm, a spring constant of <0.1 N m^{-1}, and can be used to detect thermal conductance changes of the order of 3 pW K^{-1}.

The probe was used to map the spatial change in thermal conductance of various test samples. Surface and subsurface characteristics were observed. In particular, subsurface thermal conductance variations in copper lines have been observed. Past simulations have predicted the feasibility of copper-void detection by these probes. This work reports the first experimental demonstration of thermal conductance variations in copper lines using samples provided by Sematech.

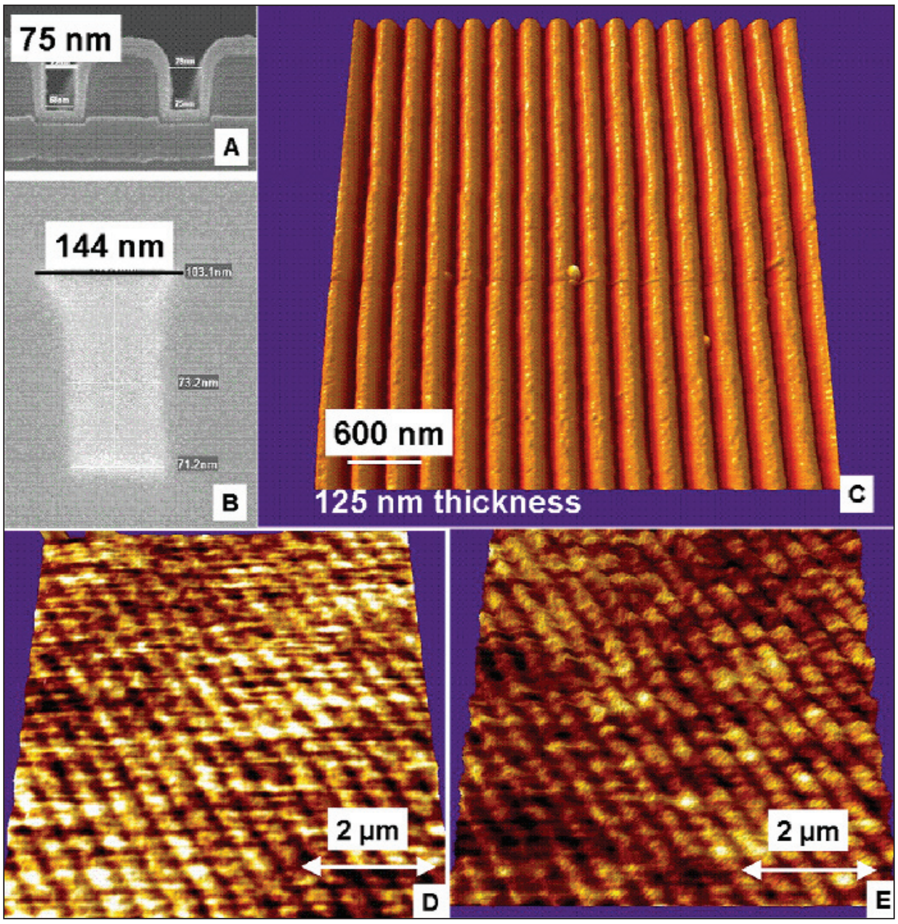

Figure 5:
(A) SEM image of cross-section of Cu line in 60-nm dense low-k dielectric film above porous low-k. Courtesy of Sematech.
(B) SEM image of trench preparation before Cu deposition. Courtesy of Sematech.
(C) AFM topographical image of Cu lines under a natural oxide 300-nm wide and 125-nm thick.
(D,E) Overlay thermal scans superimposed on topographical scans with <300 nm discontinuities in thermal conductance maps. These discontinuities occur under the natural oxide and are not visible topographically. The area scanned was 6 x 6 µm^2 and the scan rate was set at 1 Hz (D) or 1.4 Hz (E).

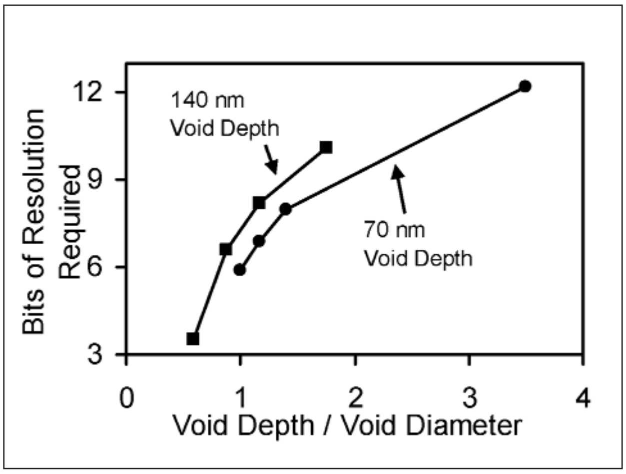

Figure 6:
The number of bits of resolution necessary to detect a void at a given depth is proportional to the ratio of the void depth to the void diameter. These simulations assume that the voids exist in a 150 nm x 150 nm x 280 nm feature of the copper, based on simulations reported in [23].

REFERENCES

1. *Li, M-H., Gianchandani, Y. B. Sensors and Actuators A 104: 236–245, 2003.*
2. *Li, M-H. et al. IEEE/ASME Journal of Micro-electromechanical Systems 10(1):3-9, 2001.*
3. *Ocola, L. E. et al. J. Vac. Sci. Technol. B, 14(6):3974-3979, 1996.*
4. *Hammiche, A. et al. Meas. Sci. Technol., 7:142, 1996.*
5. *Luo, K. et al. Appl. Phys. Lett. 68:325, 1996.*
6. *Lai, J. et al. IEEE Electron Dev. Lett. 16:312, 1995.*
7. *ThermoMicroscopes, probe model #1615-00, now part of Veeco Probes, probe model #1615-00/1610-00/CLST-NOMB.*
8. *Hammiche, A. et al. Applied Spectroscopy 53(7):810-815, 1999.*
9. *Vettiger, P. et al. IBM J. Res. Develop. 44(3):323-340, 2000.*
10. *Lerchner, J. et al. Sensors and Actuators B 70:57-66, 2000.*
11. *Majumdar A. Scanning thermal microscopy. Ann. Rev. Mater. Sci. 29: 505-585, 1999.*
12. *Williams, C. C., Wickramasinghe, H. K. Appl. Phys. Lett.49:1587, 1986.*
13. *Gianchandani Y., Najafi, K. IEEE Transactions on Electron Devices 44(11):1857-1868, 1997.*
14. *Lee, J-H. et al. International Workshop on Thermal Investigations of ICs and Systems (THERMINIC 2002), Madrid, Spain, October 2002, pp. 111-116.*
15. *Lee, J-H., Gianchandani, Y. B. Review of Scientific Instruments 75(5):1222-1227, 2004.*
16. *Basu, A. S. et al. J. Vac. Sci. Technol. B, 22(6): 3217-3220, 2004.*
17. *Hendarto, E. et al. Proceedings 43rd Annual IEEE International Reliability Physics Symposium, pp. 294-299, 2005.*
18. *Basu, A. S., and Gianchandani, Y.B. Proceedings IEEE International Conference on MicroElectroMechanical Systems, Miami Beach, FL, pp 666-669, 2005.*
19. *Basu, A. S., Gianchandani, Y. B. Presented at the 13th International Conference on Solid-State Sensors, Actuators, and Microsystems, Seoul, Korea, 2005.*
20. *McNamara, S. et al. J. Micromech. Microeng. 15:237-243, 2005.*
21. *Gaitas, A., Gianchandani, Y. B. An experimental study of contact mode scan speed constraints for polyimide cantilever probes. To be published in Ultramicroscopy, 2006.*
22. *Li, M-H. Surface Micromachined Polyimide Scanning Thermocouple and Bolometer Probes. PhD Thesis, University of Wisconsin, Madison, January 2001.*
23. *McNamara, S., Gianchandani, Y. B. Systems and Methods for Thin Film Thermal Diagnostics with Scanning Thermal Microstructures. USA Provisional Patent, Application No. unassigned, Assignee: PicoCal Inc., Filed: September 2005.*
24. *Intel Technology Journal 6(2), May 16, 2002.*

©2006 John Wiley & Sons, Ltd